

2012 EMILIA EARTHQUAKES

High-rate (1 Hz to 20 Hz) GPS coseismic dynamic displacements carried out during the Emilia 2012 seismic sequence

Antonio Avallone^{1,*}, Elisabetta D'Anastasio¹, Enrico Serpelloni¹, Diana Latorre¹, Adriano Cavaliere², Ciriaco D'Ambrosio¹, Sergio Del Mese¹, Angelo Massucci¹, Gianpaolo Cecere¹

¹ Istituto Nazionale di Geofisica e Vulcanologia, Centro Nazionale Terremoti, Italy

² Istituto Nazionale di Geofisica e Vulcanologia, Sezione di Bologna, Bologna, Italy

Article history

Received July 25, 2012; accepted September 13, 2012.

Subject classification:

Satellite geodesy, Earthquake source and dynamics, Crustal deformations, HRGPS, GPS data processing, Strong motion.

1. Introduction

In May-July 2012, Emilia Romagna (northern Italy) was struck by a significant seismic sequence, which was characterized by two moderate-magnitude earthquakes: a M_L 5.9 event on May 20, 2012, at 02:03:53 UTC, and a M_L 5.8 event on May 29, 2012, at 07:00:03 UTC, about 12 km to the west of the first mainshock. The earthquake sequence produced a total of 20 casualties and severe and widespread damage, mainly to historical and commercial buildings. A detailed description of the seismic sequence can be found in Scognamiglio et al. [2012, this volume].

The largest of the earthquake static displacements were recorded by tens of continuous global positioning system (cGPS) stations, as described in Serpelloni et al. [2012, this volume]. Most of these stations were operating with a sampling frequency of 1 Hz, and they belonged to scientific or commercial networks: RING (<http://ring.gm.ingv.it>); ITALPOS (<http://smartnet.leica-geosystems.it>); GeoTop (<http://www.netgeo.it>); Fondazione Geometri Emilia Romagna (<http://www.gpsemiliaromagna.it>; Lombardia [<http://www.gpslombardia.it>]; and Veneto (<http://147.162.229.63>). Some hours after the first mainshock, the sampling frequency of the near-field RING stations (SBPO and MODE) were switched to 20 Hz, thus recording the coseismic displacements produced by the May 29, 2012, earthquake at higher frequency. This sampling frequency was previously used for the detection of coseismic dynamic displacements only for the M_W 9 Tohoku-Oki 2011 event [Colosimo et al. 2011b]. Thus, the 20-Hz-sampling displacements for the Tohoku-Oki 2011 earthquake and the May 29, 2012, Emilia event might represent important recordings to investigate coseismic contributions at frequencies higher than 1 Hz with GPS.

In the present study, after the description of the high-rate GPS (HRGPS) data analysis, we will show and compare the preliminary results. Then, for the two mainshocks, we will

compare the displacements recorded by the HRGPS (1 Hz up to 20 Hz) and the strong-motion time histories (100 Hz) at MODE, where the different instruments were approximately co-located (Figure 1, inset, relative distance of ca. 90 m).

2. High-rate GPS data analysis strategies and results

The available HRGPS data were analyzed with two different approaches, using two noncommercial, geodetic-quality, software modules for kinematic processing: the TRACK module of GAMIT (<http://wwwgpsg.mit.edu/~simon/gtgc/>), which was developed at Massachusetts Institute of Technology; and the GD2P module of GIPSY/OASIS II (<http://gipsy.jpl.nasa.gov>), which was developed at the Jet Propulsion Laboratory (JPL, California, USA). We will briefly describe the computing strategies of these two software packages. Then, we will analyze the noise levels of each solution and the consistency of the two different solutions, by comparing the epoch-by-epoch time series of the cGPS stations located within 90 km of the epicenter and well placed along the two profiles shown in Figure 1. Finally, we will describe the peculiar MO05 results. The HRGPS data of the RING stations are available at <ftp://gpsfree.gm.ingv.it/emilia2012>.

2.1. GD2P (GIPSY/ OASIS) data-processing strategy

We used the GD2P.PL (version 6.1) module of the Gipsy-Oasis II software package [Bertiger et al. 2010], following the precise point positioning approach [Zumberge et al. 1997] in kinematic mode. With this approach, single receiver ambiguity resolution is achieved by processing dual frequency GPS data together with wide-lane phase bias estimates from a global GPS receiver network [Bertiger et al. 2010]. The same global network is used to tie in and calculate satellite fiducial orbits and clocks in the current reference frame. Thus, we used the JPL final high rate (30 s sampled)

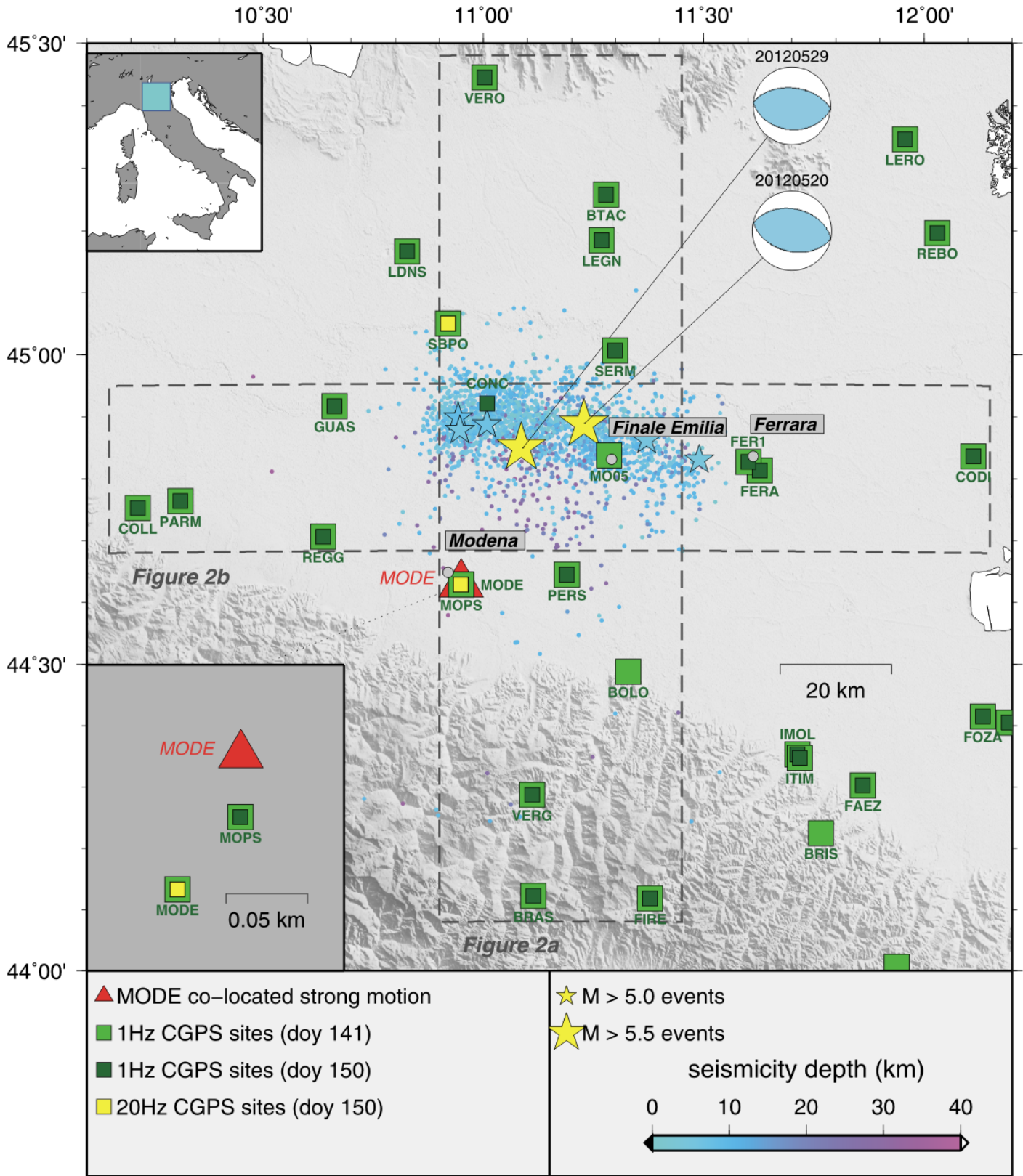


Figure 1. Locations of the high-rate (1 Hz and 20 Hz) cGPS stations operating during the Emilia-Romagna 2012 seismic sequence (squares). Red triangle, co-located strong-motion station of MODE; dashed boxes, N-S and W-E profiles of the coseismic displacements of Figure 2A, B. The two largest events (yellow stars), their focal mechanisms (beach balls), and the spatial distribution of the ca. 2300 events aftershocks (dots) are shown, as updated to July 20, 2012 (data from <http://iside.rm.ingv.it> and described in Scognamiglio et al. [2012]). The color scale indicates the depths of the aftershocks.

fiducial orbits and high rate (30 s sampled) clocks to process the code and phase the GPS data, and to obtain the epoch-by-epoch time series directly in the International Terrestrial Reference Frame (ITRF)08 reference frame [Altamimi et al.

2011]. Following Avallone et al. [2011], the satellite fiducial orbits and clocks were held fixed to estimate the receiver clocks, random walk zenith troposphere delay, and white noise receiver positions. However, with respect to Avallone et

al. [2011], two main additional aspects were applied in this study: the absolute antenna phase center corrections for the GPS receivers and transmitters, and the epoch-by-epoch ambiguity resolution [Bertiger et al. 2010].

2.2. TRACK (GAMIT) data-processing strategy

We used TRACK (version 1.27), the kinematic module of the GAMIT/GLOBK software [Herring et al. 2010], to perform epoch-by-epoch solutions of the HRGPS data and to obtain the three-dimensional time-series of the surface dynamic displacements. TRACK uses floating point LC (L3) observations and the Melbourne–Wubbena wide-lane combination, with ionospheric delay constraints, to determine integer ambiguities at each epoch, adopting Kalman-filter smoothing while estimating atmospheric delays. We use the International Global Navigation Satellite Systems (GNSS) Service (IGS) final orbits and absolute antenna phase center model. Different from the precise point positioning strategy of GIPSY, TRACK performs relative kinematic positioning, and it requires at least one reference station and one, or more, kinematic ('moving') station. For the 1 Hz data, we chose the RING site of MAGA as a fixed, 'reference', station, as it was the one with the highest data quality (i.e., low multipaths) outside the epicentral area. Having no GPS stations available outside the epicentral area with 20 Hz sampling frequency, we analyzed the higher-rate data available for MODE at 10 Hz, using as the fixed station the only 10-Hz-recording RING site, INGR. Although it has a longer baseline (MODE-INGR, 336 km) with respect to the 1-Hz solution (MODE-MAGA, 100 km), the noise level of the 10-Hz solution was comparable to the 1-Hz solutions (0.5 cm). The coordinates of the reference points are expressed in the ITRF08 reference frame.

2.3. Level of noise estimation and comparison of the HRGPS solutions

To quantify the noise levels of our HRGPS solutions, for each station and each solution, we calculated the residuals with respect to a linear fit in the 40-s time window before the earthquake. Then, we calculated the histograms of the residuals of all of the sites for the two solutions (Figure 2A). For these two earthquakes, the distributions showed that, on average, more than 96% and 72% of the residuals were within 0.5 cm for the horizontal and vertical components, respectively. These values are representative of the noise level of each solution. Moreover, to correctly compare different solutions for the same site, we also needed to quantify the consistency of each solution with respect to the other ones. Thus, we compared the May 20 and 29, 2012, HRGPS time series produced by the two analysis strategies, on two profiles (Figure 2B) that were roughly oriented in cross-strike (ca. N-S) and along-strike (ca. W-E) directions of the causative faults [Serpeloni et al. 2012].

These profiles show the variations of the waveform amplitudes at each station with the distance from the epicenter as a traditional seismic array. We considered the HRGPS time series recorded at CONC as unreliable during the May 29, 2012, event, as discussed in Serpelloni et al. [2012] for the static signal. To quantify the consistency between the GD2P and the TRACK solutions, we firstly calculated the epoch-by-epoch differences between the two solutions site-by-site. Then, we calculated the distribution of the so-determined residuals for all of the sites (Figure 2C). The histograms of these residuals show that the two solutions agree within ± 1 cm accuracy. Thus, although significantly different, the differences in the parameter tuning and, in general, in the processing strategies did not significantly affect the observations of the coseismic dynamic displacements. This comparison indicates two additional aspects.

First, the N-S and W-E profiles clearly show the propagation of the seismic waves generated by the occurrence of the May 20, 2012, M_L 5.9 earthquake and the May 29, 2012, M_L 5.8 earthquake, the epicenters of which are given in Figure 1. The waveform amplitudes reached the noise level (ca. 3 mm) at stations located at a distance greater than 60 km from the epicenter. Furthermore, considering the stations located approximately at the same distance from the epicenter, but on opposite sides (Figure 2A, SERM and PERS; Figure 2B, GUAS and FERA-FER1), there appeared to be significant differences in the waveform amplitudes for the May 20, 2012, event. This difference might be related to a source directivity effect, and we will investigate this more rigorously and in more detail in future studies. In contrast, it is of note that there were no differences in the waveform amplitudes for the May 29, 2012, event.

Second, the north component of MO05 for the May 20, 2012, event shows an initial displacement of about 50 cm peak-to-peak before this quickly decreased in amplitude until the noise level (Figure 2B). The first preliminary investigations have been performed to understand if this large displacement is reliable. The MO05 antenna was mounted on a 1-m-tall steel rod that was anchored to the top of the southward side of a school building in Finale Emilia, a village very close (6 km) to the epicenter. The side of the building where the antenna was located was not affected by macroscopic fractures or fissures, and neither liquefactions nor other local effects of the coseismic shaking were observed at its base. Minor damage might have been localized in the points where the steel rod was fixed to the building, making the mounting less stable. However, if this were the case, an increase in the noise level in the MO05 time series would be expected. Instead, the noise level before and after the mainshock that occurred and was recorded by the GD2P and TRACK solutions spanning a 350-s time interval (Figure 2D) remained unchanged on the

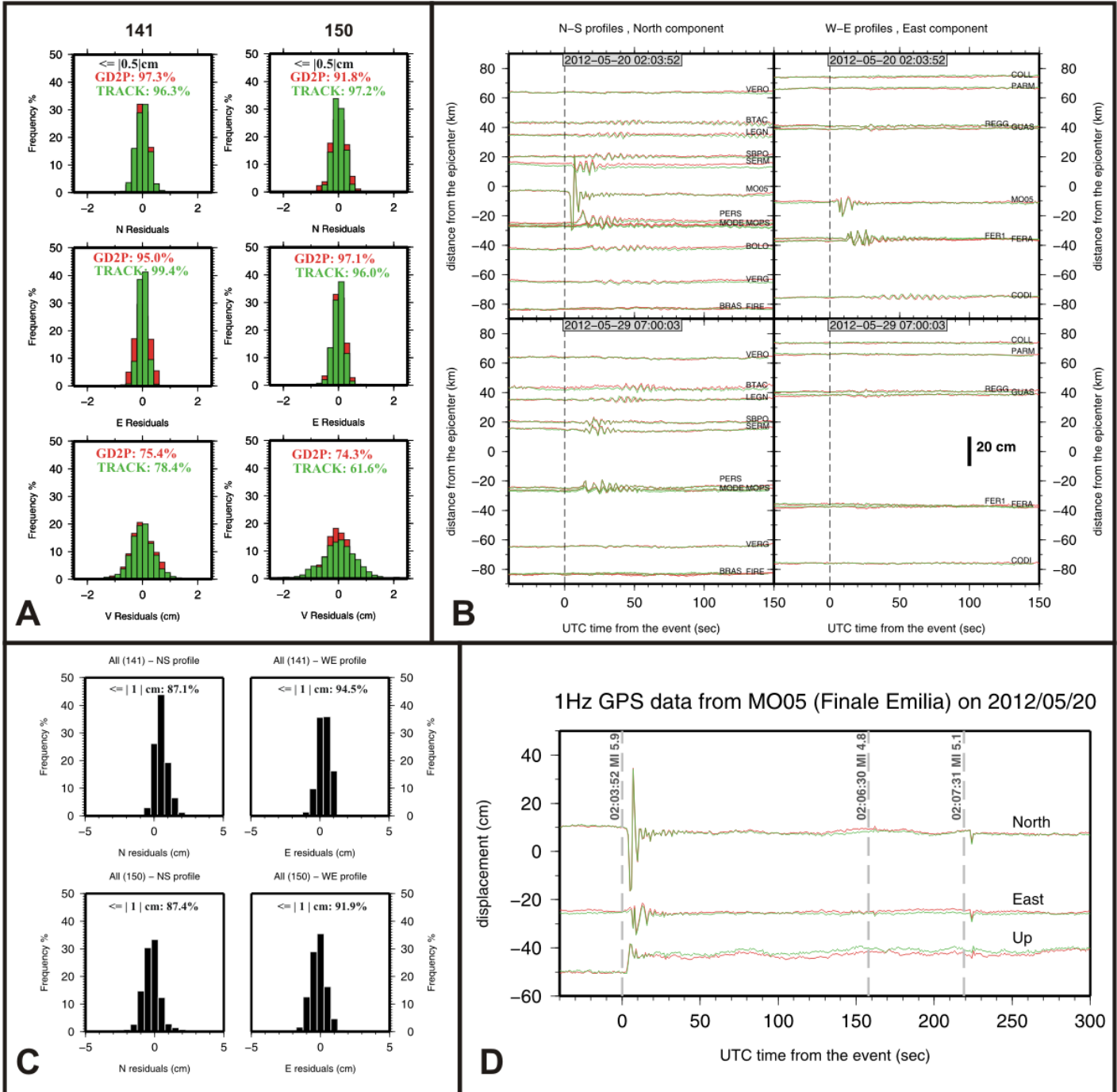


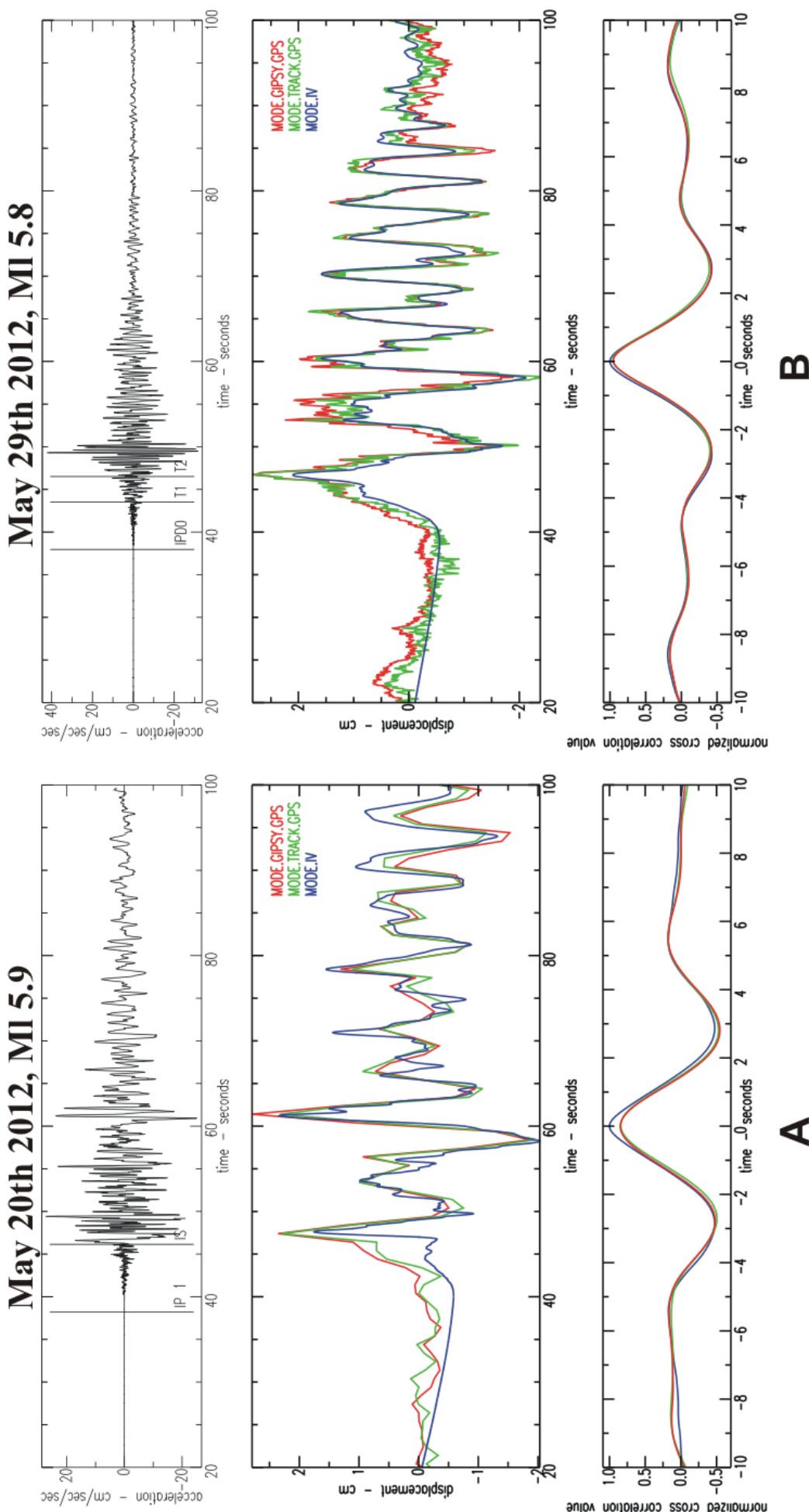
Figure 2. A. Distribution of the residuals of all of the time series in a pre-seismic 40-s time window for GD2P (red) and TRACK (green). B. North (left) and East (right) components of the 1-Hz GD2P (red) and TRACK (green) time series of sites located along the N-S and W-E profiles, respectively, of Figure 1, in a time interval of 190 s spanning the May 20, 2012, M_L 5.9 (top) and May 29, 2012, M_L 5.8 earthquakes (bottom). C. Distributions of the residuals obtained by the epoch-by-epoch difference between the GD2P and TRACK solutions on the North (left) and East (right) components. These histograms include the residuals of all of the sites of the two profiles in (B) for the May 20, 2012, event (doy 141, top) and the May 29, 2012, event (doy 150, bottom). D. Detailed comparison between GD2P (red) and TRACK (green) solutions for MO05 of May 20, 2012. The time series spans a time interval of 350 s. Dashed vertical bars, occurrence of the May 20, 2012, mainshock and of the two immediately successive aftershocks.

three components. The low noise level at MO05 allowed us to also detect the small coseismic dynamic displacements related to the two aftershocks immediately following the May 20, 2012, event. Whether the observed displacements at MO05 are directly related to the ground movement or to amplification effects due to the building oscillations is still unclear. This last aspect will be further investigated in the near future.

3. HRGPS and strong motion

Previous studies [Larson et al. 2003, Bock et al. 2004, Ohta et al. 2006, 2012, Bock et al. 2011, Colosimo et al. 2011a] have shown that GPS can detect seismic waves (both body and surface waves) for large earthquakes, and that HRGPS position time series are comparable to strong-motion data. In the case of the M_W 6.1 L'Aquila 2009 earthquake, Avallone et al. [2011] showed that the 1-cm accuracy

Figure 3. Comparison between the HRGPS solutions and the strong-motion time series at the MODE site for the May 20, 2012, $M_L 5.9$ (left) and May 29, 2012, $M_L 5.8$ (right) earthquakes. Top: north component of the strong-motion record, in acceleration, with the picking of the first arrivals. Center: comparison, in displacement (north component), between both the MODE GD2P (red) and TRACK (green) HRGPS solutions and 100-Hz sampling seismic data (blue). Left: 1-Hz HRGPS solutions. Right: GD2P and TRACK solutions, with 20-Hz and 10-Hz sampling frequencies, respectively. Bottom: normalized cross-correlation functions between GD2P and the strong-motion displacement (red), and between TRACK and the strong-motion displacement (green). Blue line, autocorrelation function of the strong-motion displacement.



of the HRGPS solutions allowed the detection of the first arrivals at near-field HRGPS sites also for moderate-magnitude earthquakes.

Both the May 20, 2012, M_L 5.9 and the May 29, 2012, M_L 5.8 Emilia earthquakes were recorded by co-located GPS and strong-motion instruments at the MODE station (Figure 1, inset: Modena). For the first earthquake (Figure 3A), the GPS station was acquiring data with a 1-Hz sampling frequency, whereas, for the second earthquake (Figure 3B), the GPS was operating with a 20-Hz sampling frequency. As mentioned above, for the second mainshock, 20-Hz and 10-Hz solutions were carried out by GD2P and TRACK, respectively. The strong-motion station was equipped with a Kinematic Episensor coupled with a Gaia2 digitizer (produced in the INGV laboratories), and it was recording with at 100-Hz sampling rate. On the N-S component of the strong-motion data, we marked the picking of the first arrivals (P-waves and S-waves) observed at this station (Figure 3A, B, top). Since the S-wave arrival appeared more uncertain for the second earthquake, we marked an interval within which we would suggest the S-wave was sure to have arrived (T1-T2).

To analyze the similarity between the strong-motion time series and the HRGPS solutions, we doubly integrated the strong-motion data, to obtain displacements (Figure 3A, B, center). In a short time window (20–100 s), we then corrected the strong-motion displacement drifts by removing the linear trend and subtracting the mean of the displacement. The comparison between the displacement waveforms was obtained by cross-correlating both the HRGPS solutions with the strong-motion data (Figure 3A, B, bottom). For the May 20, 2012, event, the normalized cross-correlation functions revealed correlation coefficients of 0.85 and 0.84 for GD2P and TRACK, respectively. Considering the maximum value of 1 (autocorrelation of strong motion), we can affirm that the cross-correlations show a relatively good match between the different solutions. For the May 29, 2012, event, the normalized cross-correlation functions showed even better correlation coefficients (0.95 for GD2P, and 0.96 for TRACK), potentially due to the higher sampling frequency, and then better similarity, of the HRGPS solutions.

In correspondence with the P-wave and S-wave arrivals on the displacement time series, we can observe a significant variation either in amplitude or frequency in both the HRGPS waveforms, in good agreement with the strong-motion data. This observation confirms the possibility that HRGPS can detect the arrival of the body waves. In Figure 3B, the sampling rate of the HRGPS solutions was higher than in Figure 3A, and different between each other (20 Hz for GD2P, 10 Hz for TRACK). However, no additional features appear to be present in the 20-Hz solution with respect to the 10-Hz solution.

4. Conclusions

The 1-Hz sampling coseismic GPS displacements were observed for the seismic wave propagation related to the two mainshocks of the Emilia-Romagna 2012 seismic sequence. The higher sampling solutions (10 Hz and 20 Hz), as well as the strong-motion data, are dominated by low frequencies, which is mainly due to two factors: 1) the lithology that generally outcrops in the investigated area, which is characterized by a huge amount of alluvial sediments of the Po Plain that quickly attenuate the high frequencies; 2) the distance from the epicentral area (35 km).

The results of this study confirm previous studies concerning the possibility that HRGPS measurements can detect both the coseismic static displacements and the body-wave-arrival dynamic displacements, without the drawback of the bias due to double integration when strong-motion data are used [Boore 2001]. The several scientific and commercial cGPS stations in Italy, operating at high-rate (mainly 1 Hz) sampling rates, allowed us to use the GPS data as seismic data. A further effort in developing denser cGPS networks that operate with sampling intervals ≥ 10 Hz would provide helpful contributions, as well as the strong-motion data, to seismology. This applies from the study of the kinematic rupture processes of causative faults [Miyazaki et al. 2004, Yokota et al. 2009, Avallone et al. 2011, Yue and Lay 2011] to the estimation of earthquake focal mechanisms [Zheng et al. 2012]. Furthermore, in the last few years, the real-time-telemetered dense cGPS networks have allowed a move towards real-time GPS seismology [Colosimo et al. 2011a, Ohta et al. 2012] for earthquake early warning [Bock et al. 2011] or tsunami early warning [Blewitt et al. 2006, Sobolev et al. 2007] purposes.

Acknowledgements. We thank all of the agencies that made the GPS observations available that are used in this study. Particular thanks are addressed to Sergio Mantentuto and Leica Geosystems S.p.A. for the rapid distribution of the Italpos cGPS station 1-Hz data. We thank the Geophysics groups of the University of Siena and the University of Bologna for the maintenance of some of the local cGPS stations (such as MO05) and for the distribution of the relative data. Finally, we thank Andre Herrero for helpful discussions about the strong-motion and HRGPS time series comparisons. We thank also Giulio Selvaggi for supporting this work. The Figures were prepared using the GMT software package [Wessel and Smith 1998].

References

- Altamimi, Z., X. Collilieux and L. Métivier (2011). ITRF2008: An improved solution of the International Terrestrial Reference Frame, *J. Geodesy*, 85, 457–473; doi:10.1007/s00190-011-0444-4.
- Avallone, A., M. Marzario, A. Cirella, A. Piatanesi, A. Rovelli, C. Di Alessandro, E. D'Anastasio, N. D'Agostino, R. Giuliani, and M. Mattone (2011). Very high rate (10 Hz) GPS seismology for moderate magnitude earthquakes: The case of the Mw 6.3 L'Aquila (central Italy) event, *J. Geophys. Res.*, 116, B02305; doi:10.1029/2010JB007834.

- Bertiger, W., S.D. Desai, B. Haines, N. Harvey, A.W. Moore, S. Owen and J.P. Weiss (2010). Single receiver phase ambiguity resolution with GPS data, *J. Geodesy*, 84, 327-337.
- Blewitt, G., C. Kreemer, W.C. Hammond, H.P. Plag, S. Stein and E. Okal (2006). Rapid determination of earthquake magnitude using GPS for tsunami warning systems, *Geophys. Res. Lett.*, 33, L11309; doi:10.1029/2006GL026145.
- Bock, Y., L. Prawirodirdjo and T.I. Melbourne (2004). Detection of arbitrarily large dynamic ground motions with a dense high-rate GPS network, *Geophys. Res. Lett.*, 31, L06604; doi:10.1029/2003GL019150.
- Bock, Y., D. Melgar and B.W. Crowell (2011). Real-time strong-motion broadband displacements from collocated GPS and accelerometers, *B. Seismol. Soc. Am.*, 101, 2904-2925; doi:10.17855/0120110007.
- Boore, D.M. (2001). Effect of baseline corrections on displacements and response spectra for several recordings of the 1999 Chi-chi, Taiwan, earthquake, *B. Seismol. Soc. Am.*, 91, 1199-1211.
- Colosimo, G., M. Crespi and A. Mazzoni (2011a). Real-time GPS seismology with a stand-alone receiver: a preliminary feasibility demonstration, *J. Geophys. Res.*, 116, B11302; doi:10.1029/2010JB007941.
- Colosimo, G., M. Crespi, A. Mazzoni and T. Dautermann (2011b). Coseismic displacement estimation, GIM International, May 2011, 25, 19-23.
- Herring, T., R.W. King and S. McClusky (2010). GAMIT Reference Manual, Release 10.4, Massachusetts Institute of Technology, Cambridge, MA.
- Larson, K., P. Bodin and J. Gomberg (2003). Using 1 Hz GPS data to measure deformations caused by the Denali Fault earthquake, *Science*, 300, 1421-1424.
- Miyazaki, S., K.M. Larson, K. Choi, K. Hikima, K. Koketsu, P. Bodin, J. Haase, G. Emore, and A. Yamagiwa (2004). Modeling the rupture process of the 2003 September 25 Tokachi-Oki (Hokkaido) earthquake using 1-Hz GPS data, *Geophys. Res. Lett.*, 31, L21603; doi:10.1029/2004GL021457.
- Ohta, Y., I. Meilano, T. Sagiya, F. Kimata and K. Hirahara (2006). Large surface wave of the 2004 Sumatra-Andaman earthquake captured by the very long baseline kinematic analysis of 1-Hz GPS data, *Earth Planets Space*, 58, 153-157.
- Ohta, Y., et al. (2012). Quasi real-time fault model estimation for near-field tsunami forecasting based on RTK-GPS analysis: application to the 2011 Tohoku-Oki earthquake (Mw 9.0), *J. Geophys. Res.*, 117, B02311; doi:10.1029/2011JB008750.
- Scognamiglio, L., L. Margheriti, F.M. Mele, E. Tinti, A. Bono, P. De Gori, V. Lauciani, F.P. Lucente, A.G. Mandiello, C. Marcocci, S. Mazza, S. Pintore and M. Quintiliani (2012). The 2012 Pianura Padana Emiliana seismic sequence: locations, moment tensors and magnitudes, *Annals of Geophysics*, 55 (4); doi:10.4401/ag-6159.
- Serpelloni, E., L. Anderlini, A. Avallone, V. Cannelli, A. Cavaliere, D. Cheloni, C. D'Ambrosio, E. D'Anastasio, A. Esposito, G. Pietrantonio, A.R. Pisani, M. Anzidei, G. Cecere, N. D'Agostino, S. Del Mese, R. Devoti A. Galvani, A. Massucci, D. Melini, F. Riguzzi, G. Selvaggi and V. Sepe (2012). GPS observations of coseismic deformation following the May 20 and 29, 2012, Emilia seismic events (northern Italy): data, analysis and preliminary models, *Annals of Geophysics*, 55 (4); doi:10.4401/ag-6168.
- Sobolev, S.V., A.Y. Babeyko, R. Wang, A. Hoechner, R. Galas, M. Rothacher, D.V. Sein, J. Schröter, J. Lauterjung, and C. Subarya (2007). Tsunami early warning using GPS-shield arrays, *J. Geophys. Res.*, 112, B08415; doi:10.1029/2006JB004640.
- Wessel, P., and W.H.F. Smith (1998). New, improved version of generic mapping tools released, *Eos Trans. AGU*, 79, 579.
- Yokota, Y., K. Koketsu, K. Hikima and S. Miyazaki (2009). Ability of 1-Hz GPS data to infer the source process of a medium-sized earthquake: the case of the 2008 Iwate-Miyagi Nairiku, Japan, earthquake, *Geophys. Res. Lett.*, 36, L12301; doi:10.1029/2009GL037799.
- Yue, H., and T. Lay (2011). Inversion of high rate (1 sps) GPS data for rupture process of the 11 March 2011 Tohoku earthquake (Mw 9.1), *Geophys. Res. Lett.*, 38, L00G09; doi:10.1029/2011GL048700.
- Zheng, Y., J. Li, Z. Xie and M.H. Ritzwoller (2012). 5-Hz GPS seismology of the El Mayor-Cucapah earthquake: estimating the earthquake focal mechanism, *Geophys. J. Int.*, 190, 1723-1732; doi: 10.1111/j.1365-246X.2012.05576.x
- Zumberge, J.F., M.B. Heflin, D.C. Jefferson, M.M. Watkins and F.H. Webb (1997). Precise point positioning for the efficient and robust analysis of GPS data from large networks, *J. Geophys. Res.*, 102, 5005-5018.

*Corresponding author: Antonio Avallone,
Istituto Nazionale di Geofisica e Vulcanologia, Centro Nazionale Terremoti, Roma, Italy; email: antonio.avallone@ingv.it.

© 2012 by the Istituto Nazionale di Geofisica e Vulcanologia. All rights reserved.